VLBA IMAGING OF CENTRAL ENGINES IN RADIO-QUIET QUASARS

JAMES S. ULVESTAD
National Radio Astronomy Observatory, P.O. Box O, Socorro, NM 87801; julvesta@nrao.edu

ROBERT R. J. ANTONUCCI
Department of Physics, University of California, Santa Barbara, CA 93106; antonucci@physics.ucsb.edu

AND

RICHARD BARVAINIS[1]
National Science Foundation, 4201 Wilson Boulevard, Arlington, VA 22230;
and Department of Physics, Gettysburg College, Gettysburg, PA 17325; rbarvai@nsf.gov
Received 2004 July 2; accepted 2004 November 12

ABSTRACT

We have used the Very Long Baseline Array (VLBA) to image five radio-quiet quasars (RQQs) at milliarcsecond resolution, at frequencies between 1.4 and 5 GHz. These quasars have typical total flux densities of a few millijanskys at gigahertz frequencies and are compact on arcsecond scales. The VLBA images reveal that four of the quasars are dominated by unresolved radio cores, while the fifth has an apparent two-sided jet. Typical core brightness temperatures range from 10^8 to at least 10^9 K. The compact radio morphologies and X-ray luminosities of many objects in the RQQ sample seem to indicate classical accretion onto black holes as massive as $10^9 M_\odot$, with emission physics in many ways similar to their radio-loud counterparts. Therefore, the relatively small amount of radiative energy emerging at radio wavelengths in the RQQs may simply be due to the presence of less powerful radio jets.

Subject headings: galaxies: active — galaxies: nuclei — quasars: general — radio continuum: galaxies

1. INTRODUCTION

Although quasars were first discovered by virtue of their strong radio emission, most actually fall within the "radio-quiet" class and thus are known as radio-quiet quasars (RQQs). These objects show optical characteristics similar to radio-loud quasars (RLQs), but ratios of radio/optical (Kellermann et al. 1989) and radio/X-ray emission (Terashima & Wilson 2003) are 1 to several orders of magnitude below the RLQs. RLQs and RQQs often have been thought to be distinct populations (Kellermann et al. 1989; Hooper et al. 1995), although the gap may be bridged by a significant population of radio-intermediate objects (White et al. 2000; Ho & Peng 2001). Arcsecond-scale radio emission from RQQs sometimes appears similar to that from RLQs, including the presence of relatively large double-jet radio sources (Kellermann et al. 1994; Kukula et al. 1998; Blundell & Rawlings 2001).

Regardless of the existence (or not) of two separate quasar classes, it is true that the radio/X-ray or radio/optical ratio can differ by several orders of magnitude between RQQs and RLQs. Possible reasons for this wide disparity in radio power between the two classes have been discussed for a number of years without a clear consensus. Some RQQs show a high-frequency excess, with apparent flat or inverted radio spectra at gigahertz frequencies (Antonucci & Barvainis 1988; Barvainis et al. 1996; Barvainis & Lonsdale 1997). It has been speculated that this emission might include a component due to thermal radio emission, and that this component might be related to the other differences in quasar properties. The thermal emission could be at 10^4 K, or even at a brightness temperature above 10^6 K, as has been inferred in the Seyfert galaxy NGC 1068 (Gallimore et al.

1997, 2004). However, recent work on radio variability of RQQs (Barvainis et al. 2005) suggests that in many cases, flat or inverted spectra in RQQs are a result of partially opaque synchrotron cores such as those found in RLQs. Milliarcsecond-resolution radio imaging can provide an independent test of the emission physics of RQQs and may illuminate any key differences between RQQs and RLQs. The brightness temperature corresponding to a ~5 millijansky source unresolved by the Very Long Baseline Array (VLBA) is ~10^8 K, roughly independent of frequency. Therefore, the VLBI technique provides a good filter for the presence of nonthermal radio emission.

Only a few RQQs have been imaged at milliarcsecond resolution. Blundell et al. (1996) first detected a milliarcsecond core in the RQQ E1821+643, and high brightness temperature cores later were found in a few more objects by Blundell & Beasley (1998) and Caccianiga et al. (2001). The typical brightness temperatures above 10^8 K in these cases apparently ruled out thermal emission from a disk or torus. In addition, observations by Blundell et al. (2003) suggest a brightness temperature high enough to require superluminal motion in one RQQ. The present paper reports further milliarcsecond imaging of a sample of five RQQs, including multifrequency imaging of several objects, using the VLBA. The goal was to determine whether the RQQ radio emission is dominated by nonthermal processes, or whether any RQQs might have radio properties affected by emission or absorption from a thermal gas.

2. SAMPLE SELECTION

In order to assess the milliarcsecond structure of RQQs chosen by some well-defined criteria, we began with the sample listed by Barvainis et al. (1996) and Barvainis & Lonsdale (1997). From their lists, we selected the 11 RQQs having total 5 GHz flux densities of 4 mJy or greater. Three of these objects show no cores stronger than 1 mJy in Very Large Array (VLA)

TABLE 1

Objects in the RQQ Sample

Name (1)	z^a (2)	B^a (mag) (3)	$S(5\ \mathrm{GHz})^b$ (mJy) (4)	$\alpha(1.4, 5)^b$ (5)	$F_X(2\text{--}10\ \mathrm{keV})^c$ (ergs cm^{-2} s^{-1}) (6)	X-Ray Band^c (keV) (7)	X-Ray Reference (8)
J0046+0104^d........	2.137	(18.2)	4.1	0.0	$<2.3 \times 10^{-13}$	0.2–3.5	1
J0804+6459^d........	0.148	(14.9)	11.7	−1.1	2.4×10^{-14}	0.5–8.0	2
J1219+0638^d........	0.334	(15.95)	9.1	+0.5	2.6×10^{-12}	0.1–2.4	3
J1225+2235..........	2.058	16.6	7.3	0.0	3.1×10^{-13}	0.2–3.5	1
J1316+0051..........	2.393	18.13	4.0	+0.1	$<1.4 \times 10^{-13}$	0.1–2.4	4
J1353+6345^d........	0.087	14.54	7.0	−1.5	8.1×10^{-13}	0.1–2.4	3
J1409+2618..........	0.945	16.07	5.8	−0.3	1.4×10^{-12}	0.5–10	5
J1436+5847^d........	0.033	14.19	5.1	−1.0	2.6×10^{-12}	0.2–2.4	6

[a] All redshifts and B magnitudes are taken from the online version of Veron-Cetty & Veron (2003). Magnitudes given in parentheses are derived from V magnitudes given by Veron-Cetty & Veron (2003), assuming $B - V = 0.3$, or from NED.
[b] The 5 GHz flux densities and spectral indices between 1.4 and 5 GHz are taken from the VLA observations of Barvainis et al. (1996) and Barvainis & Lonsdale (1997).
[c] The 2–10 keV X-ray fluxes in col. (6) are computed from values derived for the energy range given in col. (7), assuming that $N(E) \propto E^{-2}$.
[d] Object was observed successfully by the VLBA for the present paper. See additional discussion in text, as well as information in Table 2.
References.—(1) Wilkes et al. 1994; (2) Green et al. 2001; (3) Brinkmann et al. 1997; (4) Voges et al. 1999; (5); Reeves & Turner 2000; (6) Prieto et al. 2002.

images (Kukula et al. 1998), so we discarded them from the sample. Eight RQQs remained, four at relatively low redshift ($z \leq 0.33$) and four at considerably higher redshift ($0.94 < z < 2.4$). Properties of these RQQs are listed in Table 1. Our VLBI RQQ sample is not complete in any sense, but it is subject to the heterogeneity present in the original selection by Barvainis et al. (1996) and Barvainis & Lonsdale (1997).

3. OBSERVATIONS AND IMAGING

We observed six of the eight members of our sample in 1999 and 2000 using the VLBA, which is described by Napier et al. (1993); the two other RQQs had been observed previously with the VLBA (Blundell & Beasley 1998; Blundell et al. 2003). J1219+0638 and J1353+6345 also were imaged by Blundell & Beasley (1998), but we observed them at multiple frequencies to derive spectral information useful for constraining their emission processes. Table 2 summarizes the VLBA observations. In most cases, all 10 VLBA antennas participated successfully.

However, data and/or antennas were occasionally removed because of snowstorms, radio-frequency interference, or instrumentation failures.

All target quasars were below the flux density threshold needed to solve for instrumental and atmospheric effects, so each was phase referenced (Beasley & Conway 1995) to a nearby strong compact radio source. Phase-reference cycle times were 4–5 minutes, and total on-source times ranged from 1 to 4 hr per frequency band. Charged-particle effects were corrected with global ionospheric models[2] using the Astronomical Image Processing System (AIPS; Greisen 2003). Amplitudes were calibrated using standard gain files, as well as system temperatures measured at 1–2 minute intervals, then checked by observations of simple strong sources. Global clock offsets were found from observations of strong sources, while atmospheric and electronic

---

[2] Ionospheric models are available from http://cddis.gsfc.nasa.gov.

TABLE 2

VLBA Observations

Name	Date	Reference Source	Frequency (GHz)	Polarization^a	Integration (minutes)	rms^b (μJy beam^{-1})	Beam^c (mas)	P.A. (deg)
J0046+0104...........	1999 Feb 24	J0049+0237	4.99	LCP	55	107	3.8 × 2.0	17
J0804+6459...........	1999 Feb 24	J0756+6347	1.67	LCP	154	71	6.3 × 4.8	49
J0804+6459...........	1999 Feb 24	J0756+6347	4.99	LCP	235	67	2.1 × 1.6	37
J1219+0638...........	2000 Jan 21	J1222+0413	1.42	LCP	125	77	11.5 × 5.4	−2
J1219+0638...........	2000 Jan 21	J1222+0413	2.27	RCP	124	102	7.0 × 3.3	−6
J1219+0638...........	2000 Jan 21	J1222+0413	4.99	LCP	152	76	3.2 × 1.5	−8
J1316+0051^d.........	2000 Mar 12	J1256−0547	4.99	LCP	50	...	...	...
J1353+6345...........	2000 Feb 6	J1344+6606	1.42	LCP	135	90	6.6 × 5.4	4
J1353+6345...........	2000 Feb 6	J1344+6606	2.27	RCP	129	95	4.0 × 3.3	−9
J1353+6345...........	2000 Feb 6	J1344+6606	4.99	LCP	165	68	1.8 × 1.5	−5
J1436+5847...........	2000 Mar 12	J1510+5702	1.67	LCP	165	79	6.2 × 4.4	20
J1436+5847...........	2000 Mar 12	J1510+5702	4.99	LCP	228	66	2.1 × 1.4	1

[a] LCP: left-circular polarization; RCP: right-circular polarization.
[b] The noise level quoted is that for the naturally weighted data, providing the best possible sensitivity.
[c] The beam sizes given are the FWHMs for data weighting optimizing the combination of resolution and sensitivity.
[d] Imaging of J1316+0051 failed, probably because of an excessive distance of 8° from the phase-referencing source.
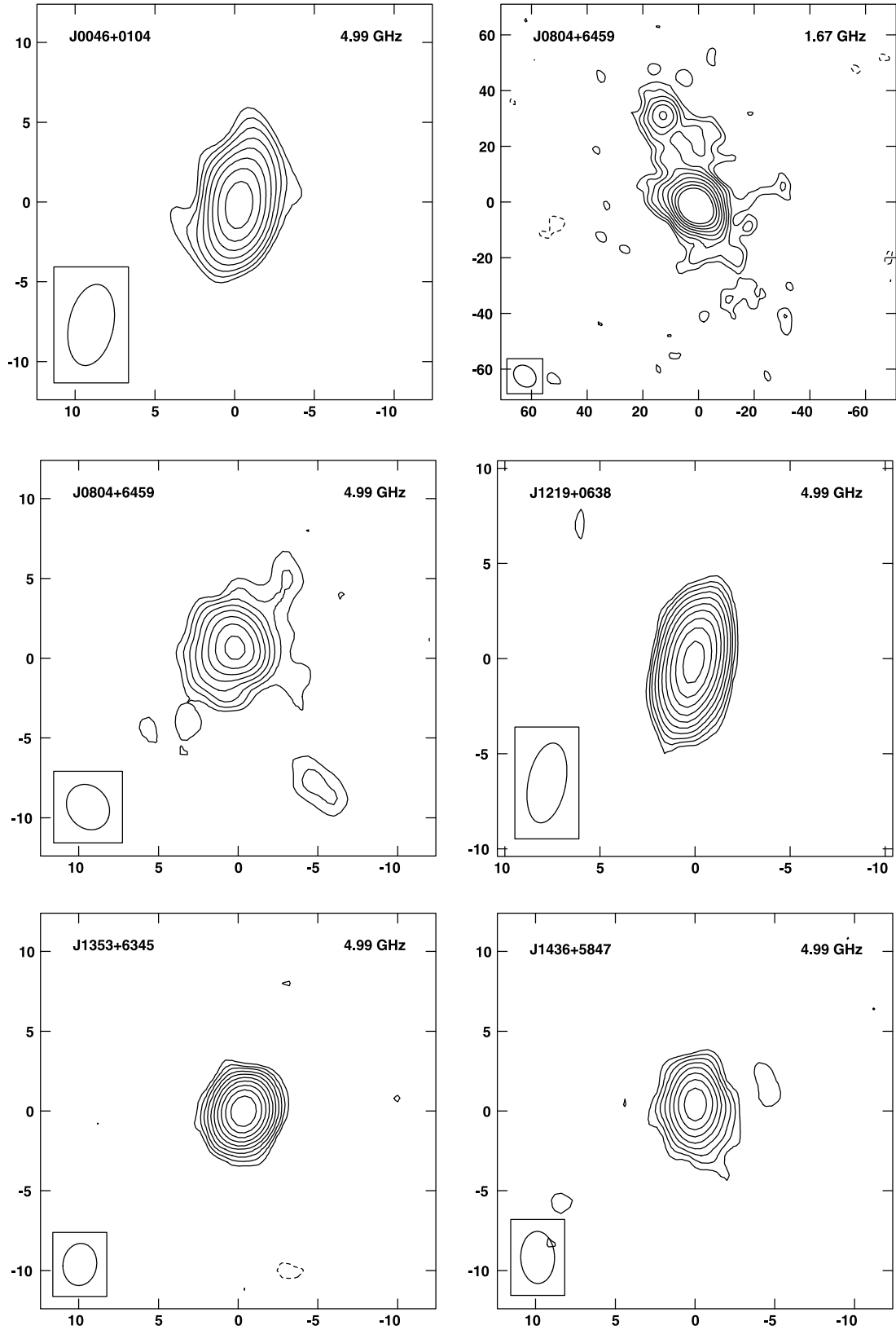
FIG. 1.—VLBA images of five RQQs imaged in our program, all in left-circular polarization at 1.67 or 4.99 GHz. The quasar names and observing frequencies are given inside each individual panel, with axes labeled in milliarcseconds referenced to the centers of the displayed images. All images are naturally weighted, with the contour levels separated by factors of $\sqrt{2}$, beginning at 3 times the rms noise given in Table 2. Negative contours are shown dashed, and half-power beam sizes are shown in the lower left corners.

TABLE 3
MEASURED PROPERTIES OF RQQs

Name	Frequency (GHz)	R.A. (J2000.0)[a]	Decl. (J2000.0)[a]	S_ν (mJy)	P_ν(em)[b] (W Hz^{-1})	T_B (rest)[c] (K)
J0046+0104........	4.99	00 46 13.5477	01 04 25.723	4.7 ± 0.5	5.3×10^{25}	$>5.6 \times 10^{8}$
J0804+6459........	1.67	...	...	24.9 ± 1.2	1.1×10^{24}	2.7×10^{8}
J0804+6459........	4.99	08 04 30.4654	64 59 52.800	6.5 ± 0.6	2.9×10^{23}	5.9×10^{7}
J1219+0638........	1.42	...	...	5.7 ± 0.3	1.6×10^{24}	$>4.5 \times 10^{8}$
J1219+0638........	2.27	...	...	7.1 ± 0.4	2.0×10^{24}	$>5.9 \times 10^{8}$
J1219+0638........	4.99	12 19 20.9317	06 38 38.467	6.4 ± 0.3	1.8×10^{24}	$>5.1 \times 10^{8}$
J1353+6345........	1.42	...	...	21.3 ± 1.1	3.4×10^{23}	$>2.4 \times 10^{9}$
J1353+6345........	2.27	...	...	14.5 ± 0.7	2.3×10^{23}	$>1.7 \times 10^{9}$
J1353+6345........	4.99	13 53 15.8307	63 45 45.686	6.8 ± 0.4	1.1×10^{23}	$>8.1 \times 10^{8}$
J1436+5847........	1.67	...	...	6.0 ± 0.3	1.2×10^{22}	$>6.0 \times 10^{8}$
J1436+5847........	4.99	14 36 22.0814	58 47 39.407	3.1 ± 0.2	6.4×10^{21}	$>3.1 \times 10^{8}$

NOTE.—Units of right ascension are hours, minutes, and seconds, and units of declination are degrees, arcminutes, and arcseconds.
[a] Source positions are listed only at 4.99 GHz, since these have the lowest errors, typically 1 mas or less in each coordinate.
[b] Radio powers are quoted as the powers that were emitted at the observed frequency. K-corrections have been computed using the spectral indices between the lowest and highest VLBA frequencies, except for J0046+0104, where the VLA spectral index listed in Table 1 was used.
[c] The listed brightness temperatures are in the rest frames of the quasars, with the observed values multiplied by $(1 + z)$. For unresolved sources, the size upper limits are assumed to be half the beam sizes. For J0804+6459, the peak brightness temperatures are listed, using the beam size as the source size.

drifts were calibrated using the local phase-reference sources. Imaging of J1316+0051 failed, since the distance of 8° from the phase-referencing source prevented successful atmospheric calibration. The other quasars had phase-reference sources between 1°.5 and 4°.5 from the target. Although their peak flux densities initially were reduced by imperfect atmospheric calibration, all had enough signal for self-calibration, which largely eliminated the image degradation.

Final images were made using two different data weightings: pure "natural" weighting, which maximizes the sensitivity, and a compromise between natural and "uniform" weighting, which provides a good combination of sensitivity and resolution. J1219+0638, J1353+6345, and J1436+5847 were observed at multiple frequencies and are unresolved at all bands, while J0046+0104 also was unresolved at its only observed frequency of 4.99 GHz. J0804+6459 contains a core with weak extended emission at 4.99 GHz but a prominent jet at 1.67 GHz. The 4.99 GHz VLBA images of the quasars are shown in Figure 1, and a 1.67 GHz image also is displayed for J0804+6459.

Table 3 lists radio positions, flux densities, powers, and brightness temperatures for each quasar. For all except J0804+6459, these results come from Gaussian fits to the core components, constrained to be completely unresolved by the synthesized beams. For J0804+6459, the total flux densities were found by integrating over the significant emission in the image. Source positions have typical errors of 1 mas at 4.99 GHz, dominated by the errors in the reference source positions and generally independent of angular separation between the target and reference sources. Source positions at the lower frequencies have larger errors due to the Earth's ionosphere and therefore are not listed. Radio powers in the source frames that were emitted at our observed frequencies were computed from the flux densities using Ned Wright's cosmology calculator.[3] A flat cosmology was assumed, with $H_0 = 71$ km s^{-1} Mpc^{-1}, $\Omega_m = 0.27$, and $\Omega_\Lambda = 0.73$ (Spergel et al. 2003). The K-correction was computed using the spectral indices between the two most widely spread VLBA frequencies when we observed at multiple frequencies, or using

the VLA spectral index from Table 1 for J0046+0104. Peak brightness temperatures were computed in the source rest frames, using the formula given by Falcke et al. (1996a), modified for an elliptical Gaussian and multiplied by $(1 + z)$ to account for the source redshift:

$$T_B = 1.8 \times 10^9 (1+z) \left(\frac{S_\nu}{1 \text{ mJy}} \right) \left(\frac{\nu}{1 \text{ GHz}} \right)^{-2} \left(\frac{\theta_1 \theta_2}{1 \text{ mas}^2} \right)^{-1} \text{ K}. \quad (1)$$

Here, S_ν is the flux density at frequency ν, with θ_1 and θ_2 being the fitted full widths at half-maximum of the major and minor axes of the sources. For the unresolved sources, the upper limits to the component sizes are taken to be one-half the beam sizes; the synthesized beam size is used for the brightness temperature in J0804+6459, since its peak flux density decreases systematically with increasing resolution, and there is no conclusive evidence for a completely unresolved component.

4. DISCUSSION

4.1. Individual Source Properties

4.1.1. J0046+0104

J0046+0104 (UM 275) is a broad absorption line quasar at a redshift of $z = 2.137$. Shields et al. (2003) report a central black hole mass of $2 \times 10^9 M_\odot$, based on Hβ line widths. The single radio component is unresolved, with a flux density of 4.7 mJy, consistent with published VLA results. The observed 0.2–3.5 keV flux upper limit is $<4.1 \times 10^{-13}$ ergs cm^{-2} s^{-1} (Wilkes et al. 1994). We convert to a 2–10 keV limit and compute the radio/X-ray flux ratio $R_X \equiv \nu S_\nu (5 \text{ GHz})/F_X(2-10 \text{ keV})$ defined by Terashima & Wilson (2003), finding $R_X > 1 \times 10^{-3}$. This is in the realm occupied by radio-loud objects according to Terashima & Wilson (2003).

4.1.2. J0804+6459

J0804+6459 also is a broad absorption line quasar, at $z = 0.148$, having a much less powerful radio source than the more distant J0046+0104. It is a relatively strong *IRAS* source; a

---

[3] The online cosmology calculator may be found at http://www.astro.ucla.edu/~wright/CosmoCalc.html.

Hubble Space Telescope image of the quasar and host galaxy is shown by Boyce et al. (1996). As might be expected from its steep radio spectrum, J0804+6459 is significantly resolved by the VLBA. The position angle of its apparent two-sided radio jet changes by $\sim 30°$ between the smallest and largest scales sampled by our VLBA observations, and the maximum radio source size of ~ 80 mas corresponds to ~ 200 pc. The 0.5–8.0 keV flux density observed by *Chandra* is 4.2×10^{-14} ergs cm^{-2} s^{-1} (Green et al. 2001). Converting this to a 2–10 keV flux and using the peak VLBA flux density of 2.4 mJy at 5 GHz, we find $R_X \approx 5 \times 10^{-3}$ firmly within the class of objects with radio-loud cores.

4.1.3. *J1219+0638*

Blundell & Beasley (1998) found "structures indicative of jets" in J1219+0638, using their short VLBA observations at 8.4 GHz. However, our deeper imaging at three lower frequencies, at which such jets would be more prominent, reveals nothing except an unresolved point source. Our measured 5 GHz flux density of 6.4 ± 0.3 mJy differs from published VLA values of 9.1 ± 0.5 mJy (Barvainis et al. 1996) and 4.0 ± 0.1 (Kellermann et al. 1989). This apparent radio variability and the overall flat spectrum support the result that the RQQ is, in fact, completely unresolved by the VLBA. The rest-frame brightness temperature of more than 5×10^8 K indicates that free-free absorption or emission is unlikely to account for the spectral shape. Instead, this RQQ almost surely contains a synchrotron self-absorbed radio core. We note that a typical brightness temperature for a self-absorbed source is $\sim 10^{10}$ K or higher. This implies that the actual source diameter may be at least a factor of 5 smaller than our upper limit, or smaller than 0.2–0.3 mas (~ 1 pc at $z = 0.334$).

J1219+0638 is a relatively strong X-ray source, with an observed 0.1–2.4 keV flux of 5.2×10^{-12} ergs cm^{-2} s^{-1} (Brinkmann et al. 1997), about 2 orders of magnitude higher than J0804+6459, despite its somewhat greater distance. Therefore, the radio/X-ray ratio of 1×10^{-4} is considerably smaller, and J1219+0638 is near the boundary between radio-loud and radio-quiet objects.

4.1.4. *J1353+6345*

Surprisingly, we find no hint of resolution in the steep radio spectrum quasar J1353+6345 ($z = 0.087$), again contradicting the inference of Blundell & Beasley (1998). Our 4.99 GHz flux density is consistent with the VLA measurement by Barvainis et al. (1996), although well below a measurement by Kellermann et al. (1989), and the 1.42 GHz flux density is nearly a factor of two less than that found by Barvainis et al. (1996). The brightness temperatures for the unresolved core approach the values where we might expect synchrotron self-absorption to occur, yet we find no evidence for such absorption in the radio spectrum. Unlike J1219+0638, we therefore suspect that the angular size of the radio source in this RQQ is not much smaller than our upper limit at 4.99 GHz and is likely to be ~ 0.5 mas (~ 0.8 pc). The observed 0.1–2.4 keV flux is 1.6×10^{-12} ergs cm^{-2} s^{-1} (Brinkmann et al. 1997), implying $R_X \approx 4 \times 10^{-4}$, within the radio-loud category.

4.1.5. *J1436+5847*

J1436+5847 (Mrk 817, or UGC 09412) is the nearest object in our sample, at $z = 0.033$, and sometimes has been classified as a Seyfert 1 galaxy rather than a quasar. Its radio power of $\sim 10^{22}$ W Hz^{-1} is within the upper end of the range found for nearby classical Seyfert galaxies (Ulvestad & Wilson 1989) and Palomar Seyfert galaxies (Ho & Ulvestad 2001; Ulvestad & Ho 2001). Previous VLA observations (Ulvestad & Wilson 1984;
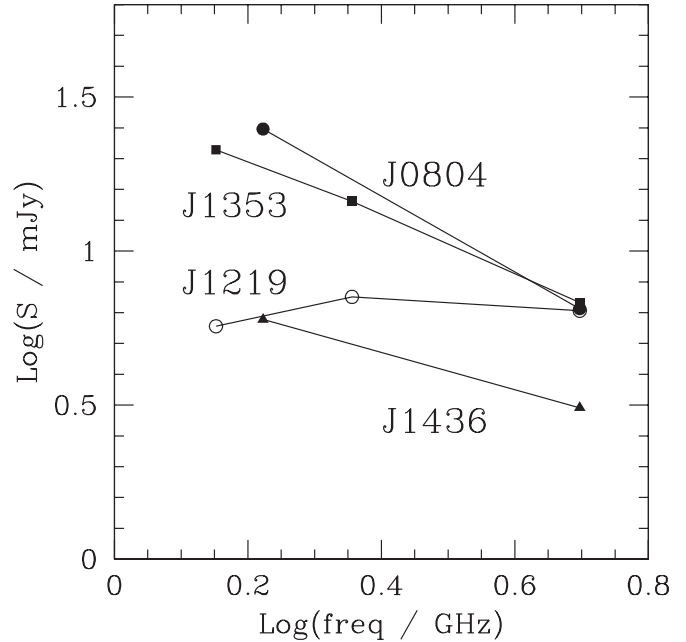

Fig. 2.—Radio spectra of the VLBI sources in four different RQQs imaged for this paper. Typical flux density errors are 0.03 dex, about the size of the plotted points.

Barvainis et al. 1996) give consistent flux densities of 5 mJy at 5 GHz, slightly higher than the value of 3.1 ± 0.2 mJy found here for the VLBI core. J1436+5847 is another steep-spectrum source that is unresolved by the VLBA and appears to be a somewhat less powerful "twin" of J1353+6345 at radio frequencies.

The 0.2–2.4 keV flux observed by *ROSAT* is 4.0×10^{-12} ergs cm^{-2} s^{-1} (Prieto et al. 2002). Converting the soft energy flux to a higher energy band, we find $R_X \approx 6 \times 10^{-5}$, putting the quasar near the border between radio-loud and radio-quiet objects.

4.2. *Source Brightness Temperatures*

Seven of the eight RQQs in the sample listed in Table 1 have now been imaged with the VLBA, so we may say something about their global properties. These objects actually have a very wide range of radio powers at 5 GHz, as expected from their similar flux densities and wide range of redshifts, yet their brightness temperature values or limits are remarkably similar. The actual values/limits are subject to a strong selection effect, namely, the fact that sources with a few millijanskys of compact flux detected on scales of one to a few milliarcseconds inevitably must have brightness temperatures of 10^8 K or greater. Still, it is a key result that essentially all the RQQs, including those with flat and steep spectra, have some components with minimum brightness temperatures of $\gtrsim 10^8$ K (see Table 3). This implies that all have nonthermal emitting cores, rather than being dominated by thermal tori such as the one inferred for NGC 1068 by Gallimore et al. (1997, 2004). Further, the four objects that we observed at multiple frequencies show no evidence for low-frequency radio turnovers, as shown in Figure 2. This implies that free-free absorption at ~ 1.5 GHz is not significant in most RQQs and thus cannot easily account for flat radio spectra at gigahertz frequencies.

4.3. *Generation of the Radio Emission*

Why do RQQs contain such compact and yet relatively low-luminosity (compared to RLQs) radio emission? A likely possibility, of course, is that this weak emission is somehow
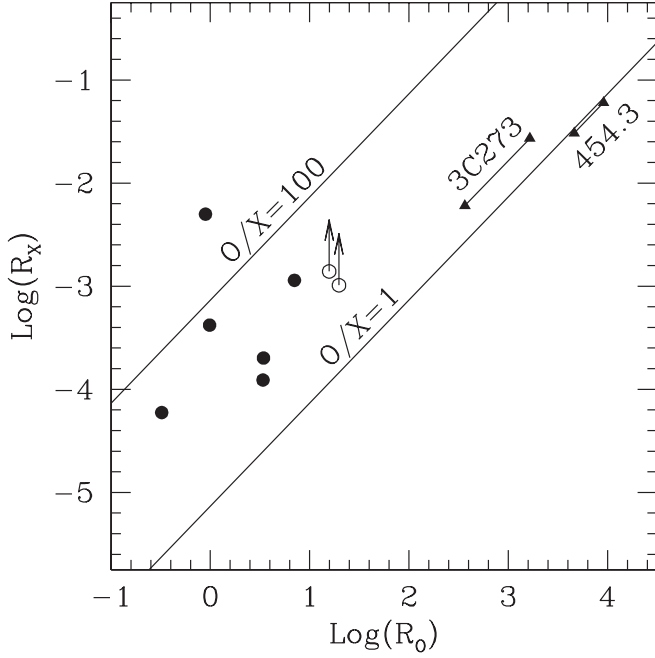
FIG. 3.— Radio/X-ray ratio R_X plotted against the radio/optical ratio R_o, for the eight RQQs in our sample. Both R_o and R_X are defined in the text. Filled circles represent objects detected at X-ray, optical, and radio wave bands, while the open circles with arrows represent the two RQQs that are not detected at X-ray wavelengths. Errors in R_X may be quite large, perhaps as high as 0.5 dex in individual cases. Diagonal lines indicate optical/X-ray ratios of 1 and 100, where the ratio is νS_ν (4400 Å)$/F_X$(2−10 keV). The RLQs 3C 273 and 3C 454.3 are also plotted, with two values corresponding to total and unresolved (by VLBI) radio flux densities.

related to the process of accretion on supermassive black holes at the centers of the quasar host galaxies, and to the efficiency of radiation from that accretion process. A key element to consider here is the overall spectral energy distributions of the RQQs. Figure 3 plots the radio/X-ray ratio versus the radio/optical ratio for the RQQs in our sample. The radio/optical ratio, R_o, is defined as the ratio of observed 5 GHz and B-band flux densities, in which the conversion from B magnitude to flux density is given by Schmidt & Green (1983). We computed the radio/X-ray ratio R_X, converting from the observed energy bands to 2−10 keV fluxes using $N(E) \propto E^{-2}$. This typically reduces the X-ray fluxes by a factor of order 2; given this fact and the lack of knowledge of the spectra, R_X values may be in error by factors of 2−3. For the five RQQs that we observed with the VLBA, the 5 GHz radio power from the unresolved milliarcsecond core has been used; otherwise, we used the total VLA flux density (see Table 1). Diagonal lines are plotted corresponding to optical/ X-ray ratios of 1 and 100, in which this ratio is defined as the ratio of νS_ν at 4400 Å to the 2−10 keV flux. The radio-loud quasars 3C 273 and 3C 454.3 are also plotted, with the two points corresponding to their total 5 GHz flux densities and the flux densities of their unresolved VLBI cores (Unwin et al. 1985; Homan et al. 2001).

Figure 3 shows some correlation between R_o and R_X, as expected, since the radio flux density appears on both axes. Most of the eight RQQs in our sample have $1 \lesssim R_o \lesssim 30$, which might be considered to indicate "radio-intermediate" quasars (e.g., Falcke et al. 1996b), and all the RQQs have $\log (R_X) > -4.5$, fitting the definition of radio-loud objects (Terashima & Wilson 2003). Of course, our choice of objects that could be observed with VLBI leads to a clear selection effect favoring relatively stronger radio sources. Since Figure 3 shows that R_X may differ

by 1−2 orders of magnitude at a given value of R_o, the implication is that the distribution of accretion energy into radiated power is very different for the individual objects. For the two RLQs plotted, the optical/X-ray ratios are somewhat lower than for the RQQs, but the strong variability of 3C 273 and 3C 454.3 makes it difficult to conclude that this might be a general trend. If it is, it could indicate an effect such as additional inverse Compton X-ray emission from strong compact VLBI jets.

We can assess further the accretion process in RQQs by taking the RQQ J1409+2618 as an example. For a black hole mass of $\sim 10^9\,M_\odot$, its Eddington luminosity would be $\sim 1.4 \times 10^{47}$ ergs s^{-1}. The B magnitude of 16.07 corresponds to an optical "luminosity" $\nu L_B \approx 5 \times 10^{46}$ ergs s^{-1}, while the X-ray luminosity is considerably weaker. Thus, the bolometric luminosity is probably close to the Eddington luminosity. Analysis for the other high-redshift RQQs in our sample gives similar results, indicating classical accretion on $\sim 10^9\,M_\odot$ black holes, consistent with results found by Vestergaard (2004). For our four RQQs with $z \le 0.33$, the lower luminosities may indicate either low radiative efficiency accretion (Narayan et al. 1998) or lower mass black holes. A number of optically selected quasars having $z \sim 0.1$–0.2 seem to contain black holes of only 10^7– $10^8\,M_\odot$ (Shields et al. 2003), favoring the latter possibility for our nearby RQQs.

Based on the above arguments and the observed brightness temperatures, we rule out either thermal processes or low-efficiency accretion for most RQQs. Why, then, are they different from radio-loud objects? One possibility could be that the radio emission in RQQs is not beamed along our line of sight. Such simple orientation schemes are ruled out, however, by the fact that RQQs do not show bright, large-scale radio structures (arcsecond- to arcminute-scale jets or double lobes) nearly as powerful as those in RLQs. An alternative scenario would have RQQ radio cores fundamentally similar to RLQs, with the RQQ jets simply being less powerful. Following Blundell & Rawlings (2001) and Barvainis et al. (2005), RQQs may produce diffuse, Fanaroff-Riley type I (Fanaroff & Riley 1974) large-scale structures as their weak jets are disrupted before escaping their host galaxies. In at least one RQQ, such a structure does exist (Blundell & Rawlings 2001), but only very deep integrations are capable of detecting these structures.

The most definitive test of a connection between RQQs and RLQs would be to achieve much more sensitive VLBI imaging in order to determine whether milliarcsecond jets are present in most RQQs, and eventually to measure the jet speeds. Blundell et al. (2003) present evidence for a Doppler factor approaching 10 for a VLBI component in the RQQ J1409+2618, one of our sample members. Direct measurement of superluminal motion, however, has yet to be achieved; we plan to search for superluminal jets in RQQs using the new High Sensitivity Array of VLBI stations.

5. SUMMARY

We have imaged five RQQs at milliarcsecond resolution using the VLBA. Four of these objects are unresolved, while a fifth shows an apparent two-sided radio jet. The brightness temperatures and spectra of the radio cores of these RQQs appear to rule out the possibility that thermal emission or absorption can be important contributors to their properties. Although the radio emission is relatively weak compared to RLQs and blazars, the overall spectral energy distributions and variability properties seem to indicate classical accretion onto black holes as massive as $10^9\,M_\odot$ for the more distant objects. The radio/ optical ratios are fairly low, but the radio/X-ray ratios of many

of our sample members actually are consistent with values for radio-loud objects. Thus, the most likely explanation for their radio properties is simply that the RQQs are similar to their "traditional" radio-loud cousins but have less powerful radio jets.

REFERENCES

Antonucci, R., & Barvainis, R. 1988, ApJ, 332, L13
Barvainis, R., Lehár, J., Birkinshaw, M., Falcke, H., & Blundell, K. M. 2005, ApJ, 618, 108
Barvainis, R., & Lonsdale, C. 1997, AJ, 113, 144
Barvainis, R., Lonsdale, C., & Antonucci, R. 1996, AJ, 111, 1431
Beasley, A. J., & Conway, J. E. 1995, in ASP Conf. Ser. 82, Very Long Baseline Interferometry and the VLBA, ed. J. A. Zensus, P. J. Diamond, & P. J. Napier (San Francisco: ASP), 327
Blundell, K. M., & Beasley, A. J. 1998, MNRAS, 299, 165
Blundell, K. M., Beasley, A. J., & Bicknell, G. V. 2003, ApJ, 591, L103
Blundell, K. M., Beasley, A. J., Lacy, M., & Garrington, S. T. 1996, ApJ, 468, L91
Blundell, K. M., & Rawlings, S. 2001, ApJ, 562, L5
Boyce, P. J., et al. 1996, ApJ, 473, 760
Brinkmann, W., Yuan, W., & Siebert, J. 1997, A&A, 319, 413
Caccianiga, A., Marchã, M. J. M., Thean, A., & Dennett-Thorpe, J. 2001, MNRAS, 328, 867
Falcke, H., Patnaik, A. R., & Sherwood, W. 1996a, ApJ, 473, L13
Falcke, H., Sherwood, W., & Patnaik, A. R. 1996b, ApJ, 471, 106
Fanaroff, B. L., & Riley, J. M. 1974, MNRAS, 167, 31P
Gallimore, J. F., Baum, S. A., & O'Dea, C. P. 1997, Nature, 388, 852
———. 2004, ApJ, 613, 794
Green, P. J., Aldcroft, T. L., Mathur, S., Wilkes, B. J., & Elvis, M. 2001, ApJ, 558, 109
Greisen, E. W. 2003, in Information Handling in Astronomy—Historical Vistas, ed. A. Heck (Dordrecht: Kluwer), 109
Ho, L. C., & Peng, C. Y. 2001, ApJ, 555, 650
Ho, L. C., & Ulvestad, J. S. 2001, ApJS, 133, 77
Homan, D. C., Attridge, J. M., & Wardle, J. F. C. 2001, ApJ, 556, 113
Hooper, E. J., Impey, C. D., Foltz, C. B., & Hewett, P. C. 1995, ApJ, 445, 62

Kellermann, K. I., Sramek, R., Schmidt, M., Shaffer, D. B., & Green, R. 1989, AJ, 98, 1195
Kellermann, K. I., Sramek, R. A., Schmidt, M., Green, R. F., & Shaffer, D. B. 1994, AJ, 108, 1163
Kukula, M. J., Dunlop, J. S., Hughes, D. H., & Rawlings, S. 1998, MNRAS, 297, 366
Napier, P. J., Bagri, D. S., Clark, B. G., Rogers, A. E. E., Romney, J. D., Thompson, A. R., & Walker, R. C. 1993, Proc. IEEE, 82, 658
Narayan, R., Mahadevan, R., & Quataert, E. 1998, in The Theory of Black Hole Accretion Discs, ed. M. A. Abramowicz, G. Björnsson, & J. E. Pringle (Cambridge: Cambridge Univ. Press), 148
Prieto, M. A., Pérez Garcia, A. M., & Rodriguez Espinosa, J. M. 2002, MNRAS, 329, 309
Reeves, J. N., & Turner, M. J. L. 2000, MNRAS, 316, 234
Schmidt, M., & Green, R. F. 1983, ApJ, 269, 352
Shields, G. A., Gebhardt, K., Salviander, S., Wills, B. J., Xie, B., Brotherton, M. S., Yuan, J., & Dietrich, M. 2003, ApJ, 583, 124
Spergel, D. N., et al. 2003, ApJS, 148, 175
Terashima, Y., & Wilson, A. S. 2003, ApJ, 583, 145
Ulvestad, J. S., & Ho, L. C. 2001, ApJ, 558, 561
Ulvestad, J. S., & Wilson, A. S. 1984, ApJ, 278, 544
———. 1989, ApJ, 343, 659
Unwin, S. C., Cohen, M. H., Biretta, J. A., Pearson, T. J., Seielstad, G. A., Walker, R. C., Simon, R. S., & Linfield, R. P. 1985, ApJ, 289, 109
Veron-Cetty, M. P., & Veron, P. 2003, A&A, 412, 399
Vestergaard, M. 2004, ApJ, 601, 676
Voges, W., et al. 1999, A&A, 349, 389
White, R. L., et al. 2000, ApJS, 126, 133
Wilkes, B. J., Tananbaum, H., Worrall, D. M., Avni, Y., Oey, M. S., & Flanagan, J. 1994, ApJS, 92, 53